Soils and Rocks
An International Journal of Geotechnical and Geoenvironmental Engineering
www.soilsandrocks.com
ISSN 1980-9743
ISSN-e 2675-5475

Açaí fiber from Amazonian waste: advanced characterization for sustainable geotechnical reinforcement applications

Augusto Barbosa Silva[1#], José Wilson dos Santos Ferreira[1], André Luís Brasil Cavalcante[1], Michéle Dal Toé Casagrande[1]

Article

Keywords
Açaí fibers
Lignocellulosic biomass
Natural fibers
Fiber treatment

Abstract

Achieving sustainable infrastructure requires the efficient valorization of regional biomass, such as açaí (Euterpe oleracea) residues. This study provides a multi-scale characterization of untreated and colloidal silica-treated açaí fibers, focusing on their application as sustainable geotechnical reinforcement. The fibers exhibit an average diameter of 0.136 mm and a naturally rough surface densely populated by silica microgranules, favoring mechanical interlocking. Chemical and lignocellulosic analyses (FTIR, XRF, and acid hydrolysis) revealed a high lignin content (45%) and moderate cellulose crystallinity (49%), indicating intrinsic robustness. However, untreated fibers showed high moisture susceptibility, with 80% absorption. The colloidal silica treatment created a stable, silicon-rich protective layer, reducing water absorption by 50% and neutralizing surface acidity, as evidenced by XRF and ash content increase to 17%. Thermogravimetric analysis by TGA/DTG demonstrated enhanced thermal stability and higher char yield for treated fibers, while tensile testing revealed a favorable balance between strength (≈250 MPa) and ductility (7.8% elongation). By bridging the gap between fiber micro-geometry and geotechnical requirements, these results demonstrate that treated açaí residue is a durable, high-value geomaterial for sustainable soil reinforcement in tropical environments.

1. Introduction

Achieving sustainable infrastructure today requires far more than simply reducing the consumption of cement or steel. In geotechnical contexts, it also demands the efficient management of regional biomass streams that would otherwise overload landfills or disrupt natural ecosystems (Boudali et al., 2022; Bai et al., 2023; Li et al., 2024). Among these streams, tropical agro-industrial residues deserve particular attention due to their large volume and limited technological valorization. Particularly within the Amazon biome, the rapid expansion of açaí (Euterpe oleracea) production not only exemplifies this challenge but also offers relevant opportunities for the valorization of the resulting biomass (Balboni et al., 2019; Buratto et al., 2021; Polidori et al., 2024).

Brazil harvested approximately 1.7 million tons of açaí in 2023 alone, with about 95% of this production concentrated in the Northern Region. In this context, the state of Pará—host of COP30—stands out as the country's leading producer, accounting for the largest share of national production (IBGE, 2025). Considering that the edible pulp represents only about 15% of the total fruit mass, approximately 85%—comprising seeds and fibrous mesocarp—remains as residual biomass after processing. This byproduct corresponds to more than one million tons of organic waste annually, imposing significant logistical and environmental challenges on local producers (Almeida et al., 2017; Bufalino et al., 2018). Converting this abundant residue into higher value-added inputs could mitigate pressures associated with waste management while simultaneously promoting the use of locally sourced materials within regional supply chains (Sato et al., 2019).

Within this scenario, the use of natural fibers derived from agricultural residues emerges as a technically promising pathway for sustainable geotechnical applications. These fibers have the potential to replace synthetic materials traditionally employed in soil reinforcement, contributing to reduced environmental impacts and enhanced valorization of residual streams (Rocha et al., 2022; Nguyen & Indraratna, 2023). Such lignocellulosic fibers offer advantages including low density, biodegradability, and mechanical properties comparable to synthetic alternatives (Pickering et al., 2016; Bordoloi et al., 2017), making them particularly suitable for geotechnical applications such as fiber-reinforced soils in landfills and low-impact earthworks. Their effectiveness fundamentally depends on the fiber–matrix interfacial interaction, governed by

[#]Corresponding author. E-mail address: augusto0412@hotmail.com
[1]Universidade de Brasília, Departamento de Engenharia Civil e Ambiental, Brasilia, DF, Brasil.

Submitted on January 21, 2026; Final Acceptance on April 22, 2026; Discussion open until November 30, 2026.
Editor: Renato P. Cunha
https://doi.org/10.28927/SR.2026.001026

factors such as surface roughness, chemical composition, and hygroscopic behavior (Han et al., 2018; Vincenzini et al., 2021). The natural surface topography favors mechanical interlocking with soil particles, while the hydrophilic nature of the fibers facilitates bonding in cementitious matrices, although it requires appropriate control in moisture-sensitive environments (Ali et al., 2016; Hassanpour & Karbhari, 2024).

This has led to growing interest in utilizing Amazonian agro-extractive residues, such as açaí waste, to create sustainable construction materials with enhanced mechanical, thermal, and environmental performance (Azevedo et al., 2021; Rocha et al., 2022; Oliveira et al., 2024; Leite-Barbosa et al., 2024). Previous studies involving açaí fibers have primarily focused on energy applications (Bufalino et al., 2018; Sato et al., 2019), cementitious composites (Azevedo et al., 2021; Natalli et al., 2024), and reinforcement of polymer matrices (Martins et al., 2008; Tavares et al., 2020), establishing basic mechanical and thermal properties. However, a comprehensive characterization aligned with the specific requirements of geotechnical applications—including surface morphology, crystallinity, water absorption kinetics, interfacial properties, and thermal stability under field conditions—remains limited. Consequently, it has not yet been clearly established whether açaí fibers meet, in an integrated manner, the performance and durability requirements imposed by real geotechnical applications, thereby hindering informed material selection and optimization of their use (Lopes & Casagrande, 2022; Santos et al., 2022).

Surface treatments represent an effective strategy to modify fiber–matrix interactions through chemical functionalization or physical coating. Among these approaches, silica-based treatments have demonstrated potential by creating hydrophobic barriers while simultaneously enhancing interfacial bonding through the formation of siloxane linkages, thereby increasing durability in moisture-exposed environments (Signorini et al., 2018; Hasanzadeh et al., 2022). The application of colloidal silica enables its penetration into the fiber microstructure, promoting the formation of Si–O–cellulose bonds that reduce water absorption without compromising surface roughness, a key feature for mechanical interlocking with soil (Zhu et al., 2019; Maia et al., 2022). However, despite the proven efficacy of silica coatings in other composites, their specific impact on the açaí fiber–soil matrix interface remains largely unexplored. Crucial aspects, such as the extent to which colloidal silica modifies the intrinsic micro-roughness of açaí fibers, its efficiency in neutralizing surface acidity for compatibility with alkaline soils, and the resulting moisture resilience under geotechnical conditions, have not yet been systematically evaluated. Addressing these specific interface unknowns is essential before validating treated açaí fibers as reliable geotechnical reinforcements.

In this context, the present study provides a systematic characterization of untreated and colloidal silica-treated açaí fibers, focusing on their subsequent application as sustainable geotechnical reinforcement. Unlike previous works, this research integrates physicochemical, mechanical, and hygroscopic analyses from a perspective directly aligned with the requirements of geotechnical engineering. The specific objectives include: (i) characterizing surface morphology and dimensional variability to assess mechanical interlocking potential; (ii) determining intrinsic physical and microstructural properties, including density and lignocellulosic composition; (iii) evaluating moisture susceptibility and the effectiveness of the silica coating in enhancing hydro-repellency; (iv) analyzing surface chemistry and mineralogical modifications induced by the treatment; (v) investigating thermal stability under degradation conditions; and (vi) assessing the balance between tensile strength and ductility to ensure mechanical compatibility with soil deformations. The results aim to demonstrate the suitability of açaí fibers for sustainable soil reinforcement in geotechnical applications, providing a comprehensive technical foundation for the valorization of this abundant agro-industrial residue.

2. Materials and methods

2.1 Materials

Natural fibers of açaí (Euterpe oleracea) were recovered from waste generated during the extraction of the açaí fruit in Belém, Pará, Brazil. The açaí fibers (Figure 1) were provided by a company that processes açaí-seed biomass. They mechanically separate the fibrous mesocarp from the endocarp through continuous drying at 300 °C inside large, rotating steel drums. At the industrial scale, this high-temperature exposure is required to rapidly arrest the natural fermentation of the moist biomass and to embrittle the physical adherence between the fibers and the hard seed, facilitating their effective mechanical detachment.

Figure 1. Açaí seed fibers.

The fibers are a residual by-product typically discarded after pulp extraction; however, the company repurposes this material by marketing it either as an organic fertilizer or by pressing it into various wood-based artifacts.

In the present study, fibers were analyzed in untreated and surface-treated conditions. Surface modification aimed at improving durability and resistance to biodegradation was carried out using colloidal silica (LUDOX® TM-50, 50 *wt*% SiO_2, Sigma-Aldrich). The treatment protocol was adapted from hydrophobization methods previously applied to lignocellulosic fibers (Silveira et al., 2022), incorporating immersion procedures reported for silica-nanoparticle dip-coating of natural fibers (Nguyen-Tri et al., 2019; Hasanzadeh et al., 2022; Maia et al., 2022).

Guided by established protocols for silica coating of natural fibers, which recommend reducing the concentration of commercial colloidal suspensions to balance coating thickness and preserve fiber flexibility (Signorini et al., 2018; Silveira et al., 2022), two dilution ratios with distilled water (1:1 and 1:2) were preliminarily evaluated. The immersion time was fixed based on the saturation period determined in the water-absorption test to ensure uniform penetration of the solution into surface voids. Air-dried fibers were weighed (±0.001 g), fully submerged, removed after immersion, lightly blotted to remove excess solution, and oven-dried at 60 °C until constant mass. Fibers treated with the 1:2 dilution adhered to each other after drying, becoming rigid and brittle, whereas fibers treated with the 1:1 dilution remained loose and flexible. Consequently, the 1:1 dilution was adopted for all subsequent analyses.

2.2 Physical and microstructural properties

2.2.1 Morphology and geometry

Fiber morphology and geometry were characterized using a Quanta 450 scanning electron microscope (SEM, FEI Company) operated at 15 kV in low-vacuum mode (10,200 Pa). Prior to imaging, fibers were sputter-coated with gold using a Q150R ES Plus system (Quorum Technologies). ImageJ software (Schneider et al., 2012) was employed to delineate fiber contours and quantify length, diameter, and cross-sectional area. This procedure follows established methodologies for dimensional characterization of lignocellulosic fibers using SEM and image analysis (Kargarzadeh et al., 2012; Liu et al., 2019).

2.2.2 Specific gravity

The specific gravity of the fibers was determined by helium gas pycnometry using a Pentapyc 5200e pycnometer (Quantachrome Instruments), following ASTM D5550 (ASTM, 2023b). Measurements were performed in triplicate to ensure reproducibility.

2.2.3 Crystallinity

X-ray diffraction (XRD) analysis was performed to evaluate the cellulose crystallinity, a fundamental parameter that influences the mechanical strength, stiffness, and durability of the fibers, as well as to verify whether the surface silica treatment inadvertently altered the internal lignocellulosic core. XRD patterns were collected using a D8 FOCUS diffractometer (Bruker) with CuKα radiation in θ–2θ configuration. Analyses were conducted at 40 kV and 30 mA over a 2θ range from 10° to 70°, with an angular step of 0.05° and a scanning speed of 1° min^{-1}. The cellulose crystallinity index (*CI*) was calculated using the Segal et al. (1959) method.

2.2.4 Water absorption

Water absorption analysis was conducted because moisture susceptibility is a critical limiting factor for natural fibers in geotechnical applications, often leading to swelling and accelerated biodegradation. Triplicate 1.0 g air-dried fiber samples, untreated and silica-coated, were immersed in distilled water at room temperature and weighed after 15 and 30 min, 1, 2, 4, 8, 24, 48, 72, 96, and 120 h. Excess surface water was removed by manual spinning for approximately 2 min followed by blotting on absorbent paper. Water absorption, *A* (%), was calculated from the initial dry mass and the wet mass after immersion. Water uptake was plotted as a function of time to determine the saturation period used in designing the surface treatment.

2.3 Chemical characterization

2.3.1 Elemental composition and functional-group analysis

Chemical characterization via Fourier transform infrared spectroscopy (FTIR) and X-ray fluorescence (XRF) was conducted to evaluate the intrinsic surface chemistry of the fibers and to chemically confirm the successful deposition of the silica coating, which directly governs the fiber–soil interfacial bonding.

FTIR was performed using a Bruker Alpha II spectrometer equipped with an attenuated total reflectance (ATR) accessory. Finely cut fiber samples were pressed directly onto the ATR crystal without chemical pre-treatment. FTIR was used to identify functional groups associated with cellulose, hemicellulose, and lignin, as well as chemical modifications induced by the silica coating.

Elemental composition was quantified by XRF using a Shimadzu EDX-720HS spectrometer with Quali-Quanti software, operating at a maximum voltage of 50 kV and current of 3 mA. Fibers were oven-dried at 60 °C until constant mass, ground to fine powder, and pressed into pellets to ensure surface uniformity.

2.3.2 Lignocellulosic composition

Determining the lignocellulosic composition is essential because the relative proportions of lignin, cellulose, and hemicellulose dictate the fiber's intrinsic resistance to microbial degradation and hydrolytic attack in geotechnical environments. The lignocellulosic composition was determined in duplicate following the acid-hydrolysis protocol described by Gessner (2005). Fibers were first Soxhlet-extracted with distilled water and ethanol to remove extractives. The extracted material was then treated with 72% H_2SO_4 to hydrolyze cellulose, rinsed with hot distilled water until acid-free, and oven-dried. The residue was incinerated to constant mass. Cellulose content was calculated from mass loss after acid treatment, lignin corresponded to the remaining solid residue, and hemicellulose was determined by difference.

2.3.3 *pH*

Fiber *pH* was measured in aqueous suspension and in 1 mol L^{-1} KCl solution using a calibrated *pH* meter, following EMBRAPA guidelines (Teixeira et al., 2017). This procedure provides insight into surface acidity and potential interactions with composite matrices (Crippa et al., 2025), particularly concerning the fiber's chemical stability when exposed to alkaline soil conditions.

2.4 Mineralogical characterization

Ash content analysis was performed to quantify the inorganic mineral fraction, serving as a direct macroscopic indicator of the silica coating's effectiveness in creating an inert protective shell. Ash content was determined according to ASTM D2974-20e1 (ASTM, 2023a). Samples were combusted in a muffle furnace (Fornitec F2-DM) with a heating rate of approximately 10 °C min^{-1} up to 450 °C, maintained for 4 h. After cooling in a desiccator, ash content was calculated as the ratio between final residue mass and initial dry mass.

2.5 Thermal characterization

Thermal characterization was carried out to evaluate the degradation kinetics of the fibers, providing indirect evidence of their physical robustness against environmental weathering and verifying the enhanced stability provided by the surface treatment. Thermogravimetric analysis (TGA) and derivative thermogravimetry (DTG) were conducted using a Shimadzu DTG-60H under nitrogen atmosphere from 25 °C to 650 °C at a heating rate of 10 °C min^{-1}. Mass-loss stages associated with moisture release, hemicellulose and cellulose decomposition, and lignin degradation were identified to assess thermal stability.

2.6 Mechanical properties

Direct tensile tests were performed following ASTM C1557 (ASTM, 2020) using a Zwick 1445 universal testing machine equipped with serrated pneumatic grips and a displacement rate of 0.1 mm min^{-1}. Single fibers were mounted in paper frames (180 g m^{-2}; 70 mm × 30 mm) with a 5 mm central opening and bonded using cyanoacrylate adhesive. EVA strips (1 mm thick) were attached at the frame ends to prevent grip damage. Sixty tests were conducted, yielding fifteen valid results. This high rejection rate is typical in natural fiber testing and was governed by strict exclusion criteria to ensure data reliability and prevent bias. Specifically, tests were discarded if the fiber slipped within the bonded area, failed prematurely at the grip interface due to stress concentrations, or exhibited macroscopic handling defects prior to loading. Only specimens that ruptured cleanly within the central gauge length, strictly adhering to ASTM C1557 guidelines, were considered valid for the analysis. Frame sides were cut immediately before loading to ensure free axial tensile action.

Mechanical tests were conducted exclusively on untreated fibers to establish baseline tensile properties of the fiber core. The silica treatment produces a surface layer that primarily modifies surface chemistry and durability rather than intrinsic tensile strength, as reported for sol–gel SiO_2 and silane coatings (Signorini et al., 2018; Nasser et al., 2018; Zhu et al., 2019). Thus, untreated fiber properties provide a representative basis for evaluating reinforcement potential in geotechnical composites.

3. Analysis and results

3.1 Physical and microstructural properties

3.1.1 Morphology and geometry

SEM observations (Figure 2a–b) show that açaí fibers present an elongated morphology with a markedly heterogeneous and rough surface, densely populated by silica (SiO_2) microgranules (indicated by arrows in Figure 2a). These microstructures are irregularly distributed along the fiber surface and confer a textured topography distinct from smoother lignocellulosic fibers. Internal voids associated with lumen channels were also observed, running longitudinally along the fiber axis (Pickering et al., 2016; Mesquita et al., 2018).

The dense population of SiO_2 microgranules observed on the fiber surface distinguishes açaí fibers from many other lignocellulosic reinforcements and plays a central role in interfacial behavior. Similar silica bodies have been reported for açaí residues by Azevedo et al. (2021) and Tavares et al. (2020), and were linked to increased stiffness of the cell wall by Mesquita et al. (2018). From a geotechnical perspective, increased surface roughness enhances frictional resistance and mechanical interlocking at the soil–fiber interface, leading to higher interface shear strength and friction angles, as demonstrated in reinforced-soil studies (Han et al., 2018; Abu Qamar & Suleiman, 2022; Pathak et al., 2025; Zhang et al., 2025). The natural silica inclusions in açaí fibers therefore act as intrinsic roughness-enhancing agents, improving soil–fiber bonding through increased asperity contact and particle coordination.

Surface-treated fibers exhibited distinct coating morphologies depending on silica concentration (Figure 3a–b). The 1:1 colloidal silica dilution produced a continuous and adherent coating layer, whereas the 1:2 dilution resulted in incomplete coverage and fiber agglomeration due to excessive rigidity after drying. Based on these observations, only fibers treated with the 1:1 dilution were considered for further analyses.

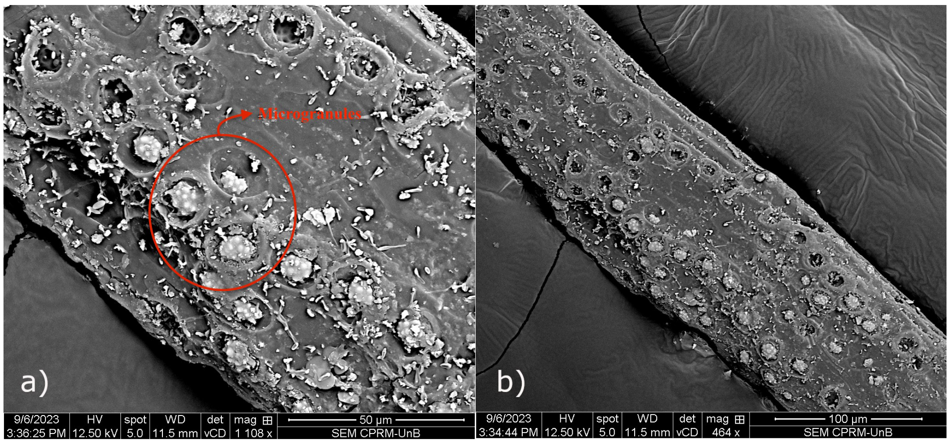

Figure 2. Morphology of açaí fibers: (A) rough surface densely populated with SiO_2 microgranules (indicated by arrows); (B) elongated morphology.

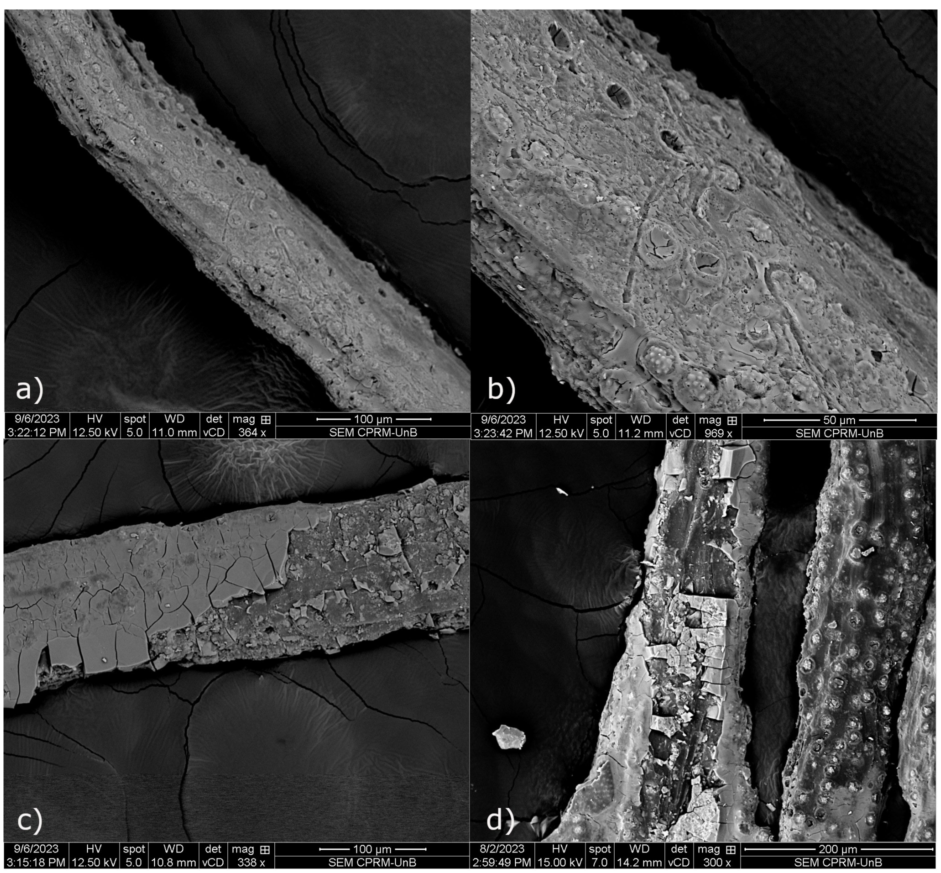

Figure 3. SEM waterproofed açaí fibers in a ratio of (A, B) 1:1; (C, D) 1:2.

Cross-sectional analysis revealed two predominant geometries: approximately cylindrical and flattened sections (Figure 4a and 4b). Transverse cuts, performed manually using a sharp surgical scalpel, also exposed elongated lumens that were frequently collapsed or distorted due to the mechanical stress of the sectioning process (Figure 4c and 4d), reflecting the typical anatomical structure of lignocellulosic fibers.

Image analysis yielded an average fiber diameter of 0.136 mm with a coefficient of variation of approximately 30%, and an average length of 9.4 mm (Table 1). The broad dispersion of dimensions reflects the natural variability of açaí fibers.

Fiber geometry further influences load transfer mechanisms. The coexistence of cylindrical and flattened cross-sections reflects the anatomical variability typical of lignocellulosic fibers and has been widely reported for natural reinforcements extracted under different growth and processing conditions (Pickering et al., 2016; Garat et al., 2018). Flattened or elliptical sections increase contact area and promote mechanical interlocking, while diameter variability affects stress transfer and pull-out resistance (Vincenzini et al., 2021; Huzni et al., 2022). In addition, the presence of elongated lumens—common in plant fibers—creates preferential pathways for water ingress, which may accelerate degradation when fibers remain untreated (Pickering et al., 2016).

Table 1. Açaí fibers dimensional parameters.

D_f (mm)	L_f (mm)	Authorship
0.136 ± 0.04	9.432 ± 2.83	Current work
0.12 ± 0.03	21.2 ± 7.5	Polidori et al. (2024)
0.11 ± 0.03	22 ± 8.7	Mesquita et al. (2018)
0.164 ± 0.052	-	de Oliveira et al. (2019)
~0.3	~25	Marvila et al. (2020)
~0.08	~20	Pessoa et al. (2010)

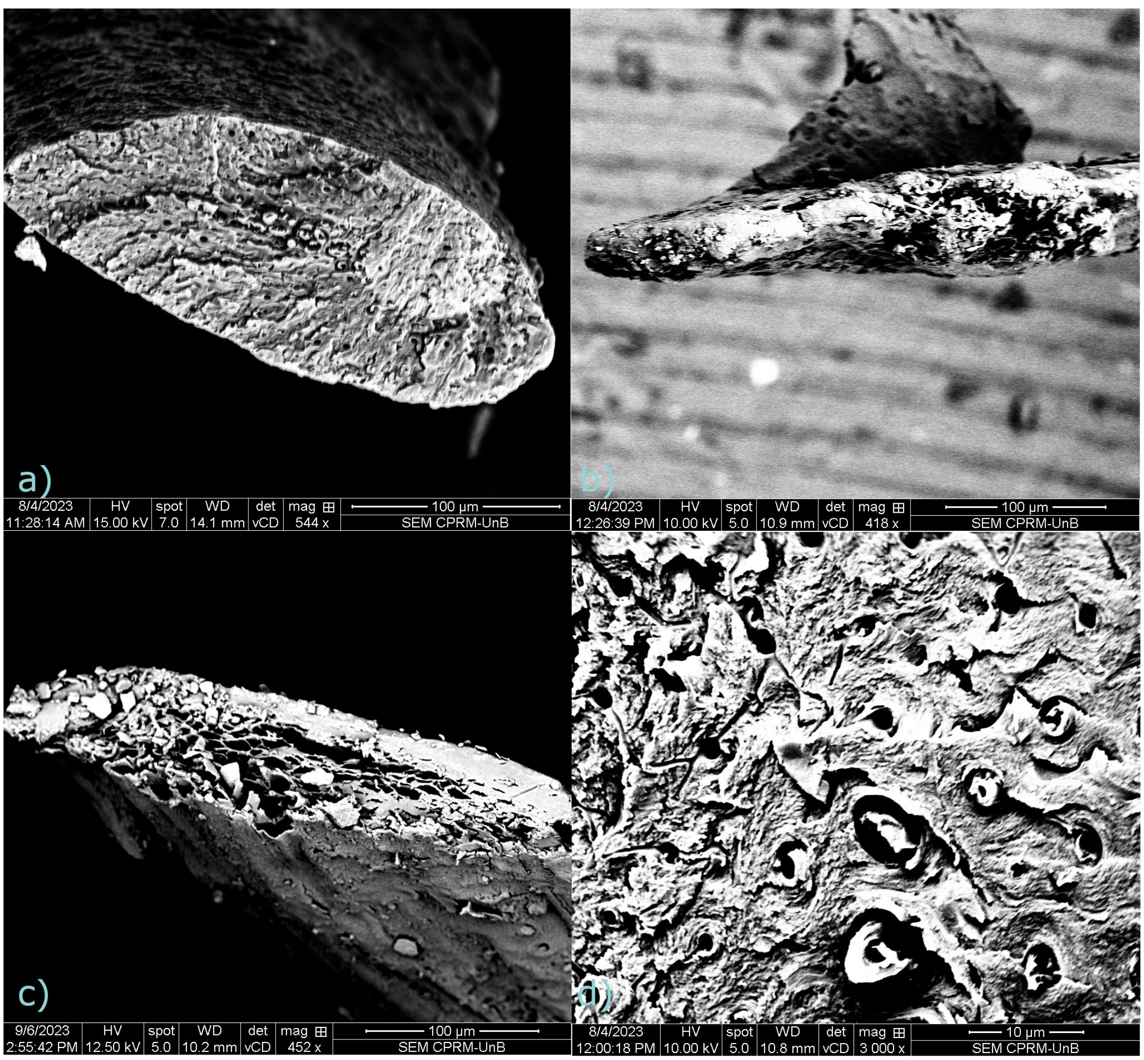

Figure 4. Recurrent cross-sectional shapes: (A) approximately cylindrical; (B) distinctly flattened. Cross section of açaí fiber: (C) general view; (D) lumens in close-up.

Such morphological heterogeneity must therefore be considered when defining fiber dimensions and mixing procedures for geotechnical applications.

3.1.2 Specific gravity

The specific gravity of açaí fibers was measured as 0.89 ± 0.03 g·cm^{-3}. This value places açaí among the lightest lignocellulosic reinforcements, confirming its lightweight nature. It is comparable to coir and significantly lighter than jute or sisal (Nguyen & Indraratna, 2023). In reinforced soils, this characteristic is advantageous for reducing the unit weight of fills and embankments while maintaining effective reinforcement. When combined with surface roughness imparted by silica inclusions, low density does not compromise interfacial performance, but rather supports efficient stress redistribution within the soil matrix.

3.1.3 Crystallinity

X-ray diffraction patterns (Figure 5) indicate a crystallinity index (*CI*) of 47% for untreated fibers. After colloidal silica treatment, the *CI* increased to 49%, accompanied by a slight shift of the main cellulose diffraction peak from $2\theta = 22.7°$ to 22.15°. These results indicate a modest increase in crystalline order following surface treatment.

The crystallinity index of untreated açaí fibers falls within the typical range reported for plant-based reinforcements (Poletto et al., 2014; Lima et al., 2021). The modest increase in crystallinity after colloidal silica treatment is consistent with observations reported for thermally treated açaí fibers (Tavares et al., 2020) and chemically modified eucalyptus fibers (Oliveira et al., 2024), and is generally attributed to surface-level filling of amorphous regions rather than internal structural alteration. As emphasized by Cruz & Fangueiro (Cruz & Fangueiro, 2016), waterproofing treatments can modify surface characteristics without compromising the integrity of the lignocellulosic core. In this context, the primary contribution of silica coating lies in surface protection rather than intrinsic strengthening.

3.1.4 Water absorption

The water absorption behavior of untreated and silica-coated fibers is presented in Figure 6. Both materials exhibited rapid initial water uptake within the first 24 h, reaching approximately 53–54% mass gain. Beyond this period, untreated fibers continued to absorb water, reaching approximately 80% at 48 h and stabilizing thereafter.

In contrast, silica-coated fibers reached saturation within approximately 30 min and showed only minor additional uptake (<2%) over extended immersion times. Overall, long-term water absorption of treated fibers was reduced to nearly half that of untreated fibers.

Water absorption behavior highlights one of the most critical limitations of untreated natural fibers in geotechnical environments. The continued uptake of water observed in untreated açaí fibers reflects moisture migration into lumens and secondary cell wall layers, a process associated with swelling, hemicellulose leaching, and accelerated biodegradation under wet–dry cycles (Castro et al., 2022; Lv et al., 2023; Eleutério et al., 2025). The colloidal silica treatment markedly altered this behavior by limiting long-term water diffusion, stabilizing mass gain within minutes, and

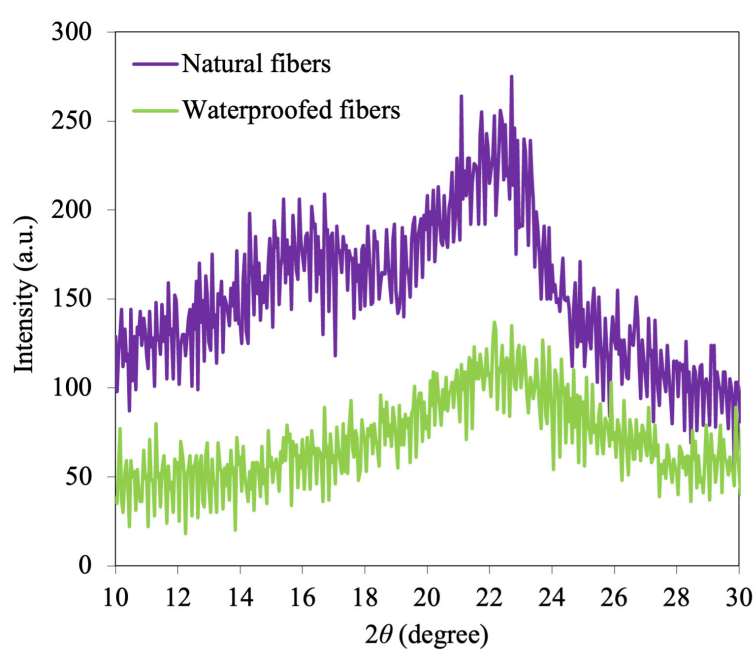

Figure 5. Intensity vs 2θ graph for crystallinity calculation.

reducing total absorption to nearly half that of untreated fibers. Similar reductions have been reported for silica-coated sisal fibers (Silveira et al., 2022) and polymer-treated Amazonian fibers (Oliveira et al., 2020). By reducing the availability of free hydroxyl groups and limiting capillary flow along the fiber surface, hydrophobic treatments effectively preserve interfacial integrity and mechanical performance under cyclic moisture exposure (Oun et al., 2022; Shifa et al., 2024).

3.2 Chemical Characterization

3.2.1 Elemental composition and functional-group analysis

FTIR spectra of untreated and silica-coated fibers are shown in Figure 7. Untreated fibers exhibited characteristic absorption bands associated with lignocellulosic materials, including broad O–H stretching (3700–3000 cm^{-1}), C–H stretching (2900–2800 cm^{-1}), C=O stretching (1740–1710 cm^{-1}), aromatic C=C vibrations (1605–1505 cm^{-1}), and cellulose-related bands in the 1200–900 cm^{-1} region.

After silica treatment, a reduction in O–H band intensity was observed, along with increased intensity in the 1200–900 cm^{-1} region, indicating surface modification. Other spectral features remained largely unchanged, suggesting preservation of the lignocellulosic core.

XRF results (Table 2) show that untreated fibers contain significant amounts of Fe, K, Si, and Ca. Following silica treatment, silicon content increased to approximately 91 *wt*%, while the relative proportions of other elements decreased accordingly, consistent with the formation of a silica-rich surface layer.

FTIR results indicate partial masking of hydroxyl groups and preservation of the lignin framework, while XRF confirms the formation of a silicon-rich surface layer.

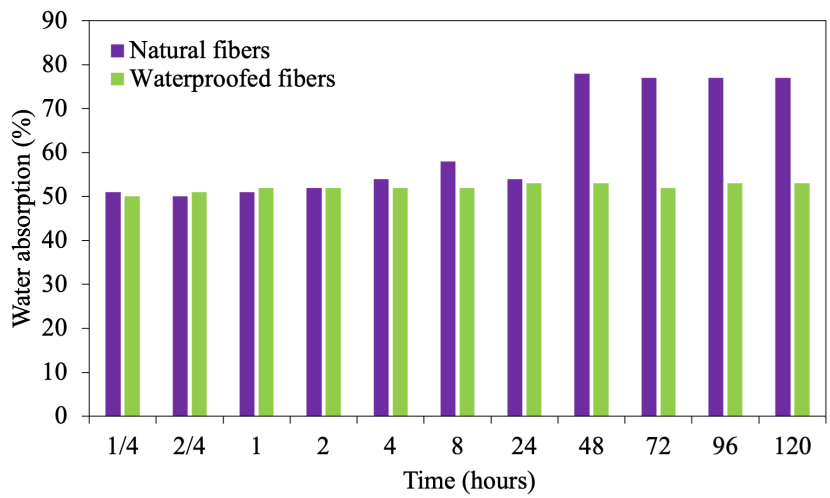

Figure 6. Graph of water absorption versus time.

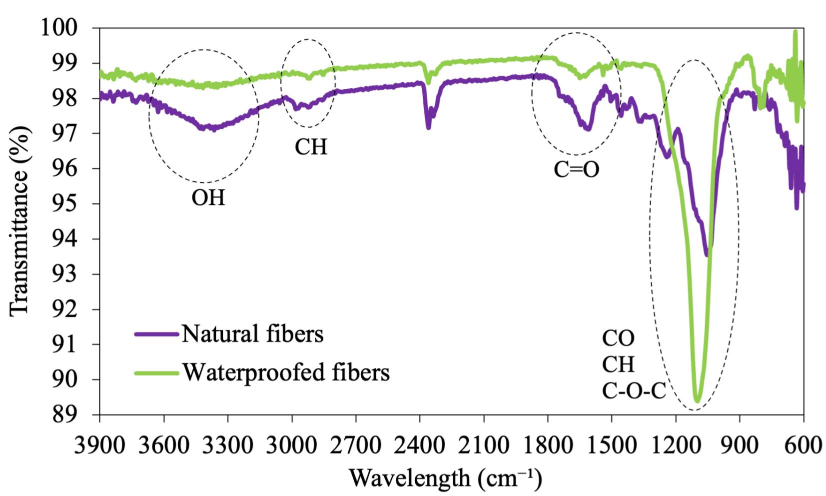

Figure 7. Fourier Transform Infrared Spectroscopy.

The substantial increase in surface silicon mirrors results reported for silica-treated sisal fibers (Silveira et al., 2022) and explains both the reduced water uptake and the increased ash content. From a durability standpoint, the SiO_2 shell acts as a chemically inert barrier that limits ion exchange with pore fluids and reduces susceptibility to microbial attack.

3.2.2 Lignocellulosic composition, *pH* and ash content

The lignocellulosic composition of açaí fibers is summarized in Table 3. The fibers exhibited cellulose, lignin, and hemicellulose contents within the ranges previously reported for açaí residues. The composition is characterized by a relatively high lignin fraction, moderate cellulose content, and comparatively low hemicellulose content.

The lignocellulosic composition of açaí fibers further enhances their durability potential. The relatively high lignin content and low hemicellulose fraction place açaí between coir and sisal in terms of resistance to hydrolytic degradation (Bordoloi et al., 2017). Hemicellulose is the most hydrophilic and unstable constituent of plant fibers, and its degradation under cyclic moisture exposure has been shown to reduce tensile strength by up to 70% in natural-fiber composites (Lv et al., 2023). Consequently, the intrinsic composition of açaí fibers provides an advantage over hemicellulose-rich reinforcements.

Regarding *pH* results, untreated fibers are slightly acidic ($pH \approx 6$), with KCl dropping 0.5 units due to surface carboxyl and phenolic groups. After coating, water-suspension *pH* rises to near-neutral (6.9) and KCl to 6.0, indicating SiO_2 neutralizes acidic sites. This is advantageous in alkaline soils by retarding proton-catalyzed hydrolysis and enhancing interface stability. Guarino et al. (2015) demonstrated that alginate remains stable only at *pH* 5–10, where proton-catalyzed hydrolysis ($pH < 5$) and β-alkoxy-elimination ($pH > 10$) are minimized, supporting neutralizing treatments to preserve fiber integrity. The negative ΔpH indicates predominant negative surface charges, enhancing soil-fiber interaction when soil has opposite charges (Crippa et al., 2025). Overall, the silica treatment creates an Si-dominant, hydrophobic shell that neutralizes acidity and reorganizes surface groups without disrupting the lignocellulosic core.

Ash testing quantifies inorganic residue after organic combustion, measuring a fiber's mineral fraction. Table 3 shows ash results for untreated and silica-coated açaí fibers. Untreated fibers contain ~2% ash, consistent with the 1–3% range for lignocellulosic reinforcements (Bilcati et al., 2018). Eleutério et al. (2025) reported similar values: cotton 0.8–2%, hemp ~0.8%, jute 0.5–2%, and sisal 0.6–1%, corroborating açaí's 2% ash content. This low fraction indicates the fiber is primarily cellulose, hemicellulose, and lignin, with minor minerals (Si, Fe, Ca, K) identified by XRF.

After silica treatment, ash rises sharply to ~17%, confirming SiO_2 deposition. This 15-percentage-point gain corroborates the 91% Si from XRF and reduced O–H intensity in FTIR. Unlike thermal treatment, which removes minerals (Tavares et al., 2020), silica coating enhances mineral surface roughness.

Geotechnically, increased mineral fraction offers two advantages: (1) durability—the inert SiO_2 shell resists microbial attack and degradation, similar to Silveira et al. (2022), who reported 20% tensile strength gains in silica-coated sisal; (2) interfacial behavior—mineralized surfaces enhance friction and interlocking with soil (Kadhim & Alyounis, 2024).

The ash results confirm silica treatment substantially modifies mineralogical composition while preserving the lignocellulosic core, supporting long-term geotechnical reinforcement.

Table 2. X-ray Fluorescence result of açaí fibers.

Element (%)	Fe	K	Si	Ca	Mn	S	Cr	P	Al	Cu	Zn	Ti
NF	27.7	20.5	20.5	14.3	5.3	4.0	2.8	2.3	1.7	0.5	0.4	-
WF	1.5	1.3	90.9	2.6	0.5	1.4	0.1	-	1.6	-	-	0.1

Note: *NF* = natural fibers; and *WF* = waterproofed fibers.

Table 3. Results of structural composition, surface pH, and ash content of untreated and silica-coated açaí fibers.

Property	Parameter	Natural fibers	Waterproofed fibers
Structural component contents	Cellulose (%)	31	-
	Hemicellulose (%)	12	-
	Lignin (%)	45	-
pH	*pH* (H_2O)	5.80	6.92
	pH (KCl)	5.28	5.96
	ΔpH (KCl – H_2O)	-0.52	-0.96
Ash content	Organic matter (%)	97.59	82.57
	Inorganic matter (%)	2.41	17.43

3.3 Thermal characterization

Thermogravimetric (TGA) and derivative thermogravimetric (DTG) curves for untreated and treated fibers are shown in Figure 8. Three main mass-loss stages were identified: an initial stage below 200 °C associated with moisture loss; a second stage between approximately 200 °C and 370 °C corresponding to hemicellulose and cellulose degradation; and a third stage extending up to 500 °C associated with lignin decomposition.

Untreated fibers retained approximately 87% of their mass at 200 °C and yielded a char residue of approximately 14% at 850 °C. Silica-treated fibers exhibited increased mass retention at intermediate temperatures and a higher final residue of approximately 29%, indicating enhanced thermal stability.

Thermal analyses provide additional evidence of the effectiveness of silica coating. The enhanced thermal stability and higher char yield reflect increased resistance to thermal and oxidative degradation. Comparable improvements in thermal behavior have been reported for chemically treated natural fibers and composites (Nurazzi et al., 2021; Neto et al., 2021), although the final effect depends on fiber–matrix interactions (El-Shekeil et al., 2012). The high char yield observed is consistent with the elevated lignin content of açaí fibers, as lignin is known to promote char formation due to its aromatic structure (Zhang et al., 2018).

3.4 Mechanical properties

From direct tensile tests, the values mean ± standard error of tensile strength, Young's modulus, and elongation at the break were determined for natural açaí fibers, which are presented in Table 4. Exhibiting a tensile strength of ≈250 MPa ± 3.55, açaí fibers match or exceed many natural reinforcements. This is only 8% lower than sisal's 271 MPa (Silveira et al., 2022) and exceeds coir's 95–230 MPa (Hasan et al., 2021; Martinelli et al., 2023), kenaf's 20–230 MPa (Huang et al., 2025; Radzuan et al., 2020), and fique's 142–262 MPa (Muñoz-Blandón et al., 2023). High lignin (45%) and moderate crystallinity (49%) account for this strength-toughness balance. Natural fiber tensile strength typically ranges 150–800 MPa, influenced by diameter, lignin, and cellulose crystallinity (Pickering et al., 2016).

The reported variability, expressed as standard error, reflects the natural dispersion typically observed in lignocellulosic fibers and should be considered when defining design safety factors in geotechnical applications. The modulus of 3.7 GPa is lower than sisal's 5.5 GPa (Silveira et al., 2022) but close to that of coir (4 ± 1 GPa). Considering that soils typically exhibit elastic moduli substantially below 1 GPa, this stiffness contrast between the reinforcement and the surrounding matrix plays a critical role in load transfer efficiency (South Carolina Department of Transportation (SCDOT, 2022). Such contrast is expected to enable more efficient stress transfer while avoiding the brittleness typically associated with high-modulus synthetic fibers, thereby promoting favorable mechanical compatibility with the soil.

Furthermore, a mean failure strain of 7.8%—approximately 50% greater than the 5.2% recorded for sisal—provides a ductile response, allowing the fibers to accommodate soil settlements and deformations without catastrophic failure. The ductility of the fibers not only enhances strain compatibility with clayey soils but also reduces the risk of sudden pull-out failure in reinforced slopes and embankments.

Table 4. Results of direct tensile tests on açaí fibers.

Tensile Strength (MPa)	Young's modulus (GPa)	Elongation at break (%)
249.72±3.55	3.73±0.33	7.83±0.70

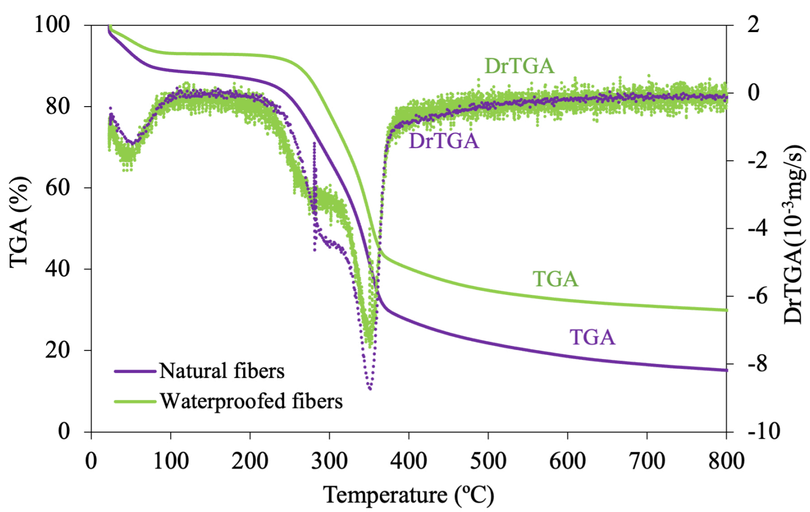

Figure 8. Thermogravimetry (TGA/DTG) results on natural açaí fibers.

The combination of moderate tensile strength and high elongation at break in açaí fibers offers an optimal balance for soil reinforcement applications, where excessive stiffness may induce stress concentrations and brittle failure. These characteristics establish açaí fiber as a robust and chemically durable reinforcement, particularly well-suited to tropical geotechnical environments, where seasonal variations in moisture content and microbial activity pose significant challenges to unprotected natural fibers.

Although the mechanical testing in this study focused exclusively on untreated fibers to establish the baseline properties of the lignocellulosic core, the application of the colloidal silica coating is theoretically expected to influence the overall composite behavior. Based on the literature regarding surface-treated natural fibers (Signorini et al., 2018; Silveira et al., 2022), the formation of a rigid SiO_2 shell does not typically alter the ultimate tensile strength of the internal fiber core. Furthermore, because the treatment successfully preserves the intrinsic surface roughness and dimensional variability of the açaí fibers, it maintains their natural capacity for mechanical interlocking within the soil matrix. Consequently, the primary influence of the silica treatment is anticipated to be related to long-term durability, protecting the fiber from hydrolytic swelling and microbial degradation, rather than a direct increase in the immediate macroscopic mechanical resistance of the reinforced soil. This ensures that the favorable baseline mechanical properties are sustained over time in challenging geotechnical environments.

4. Conclusion

This study provides a multi-scale characterization of untreated and colloidal silica-treated açaí fibers, demonstrating their potential as sustainable geotechnical reinforcements. The main findings are:

- Açaí fibers exhibit a naturally rough and heterogeneous surface densely populated by SiO_2 microgranules, which enhance soil–fiber friction and mechanical interlocking. The fibers also present low specific gravity (0.89 ± 0.03 g·cm^{-3}), making them suitable for lightweight geotechnical applications;
- The lignocellulosic composition (cellulose 31%, hemicellulose 12%, lignin 45%) indicates potential resistance to biodegradation, particularly due to the high lignin and low hemicellulose contents compared to other natural fibers;
- Colloidal silica treatment significantly improved hydro-mechanical behavior, reducing water absorption from approximately 80% to about 40% and shortening the saturation time from 48 h to 30 min, indicating effective hydrophobization of the fiber surface;
- Ash content increased from approximately 2.4% to 17.4%, and XRF analysis showed a rise in silicon content to ~91 wt%, confirming the formation of a silica-rich protective layer;
- FTIR analysis indicated partial masking of hydroxyl groups (3700–3000 cm^{-1}) and increased intensity in the 1200–900 cm^{-1} region, suggesting the formation of Si–O bonds while preserving the lignocellulosic core;
- Thermal analysis identified three degradation stages: moisture loss below 200 °C, decomposition of hemicellulose and cellulose between 200–370 °C, and lignin degradation up to 500 °C. Treated fibers showed increased thermal stability and higher residual mass (~29%);
- Mechanical properties of untreated fibers showed a tensile strength of 249.72 ± 3.55 MPa, Young's modulus of 3.73 ± 0.33 GPa, and elongation at break of $7.83 \pm 0.70\%$, indicating a favorable balance between strength and ductility for soil reinforcement applications.

Overall, the results position açaí residue as an abundant, durable, and high-value geomaterial, capable of supporting sustainable, locally sourced geotechnical solutions in tropical environments. Based on the scope and limitations of the present study, evaluation of soil–fiber interaction, such as pull-out, oedometer, and triaxial testing of the reinforced soil composite, is recommended.

Acknowledgements

The authors gratefully acknowledge the support received from the University of Brasília (UnB) and the Federal Institute of Science, Education and Technology of Rondônia (IFRO). Also, authors gratefully acknowledge the financial support provided by Coordination for the Improvement of Higher Education Personnel (CAPES), Brazilian National Council for Scientific and Technological Development (CNPq), and Research Support Foundation of the Federal District (FAP/DF) under Project SEI-GDF No. 00193-00001386/2024-04.

Declaration of interest

The authors declare that they have no known competing financial interests or personal relationships that could have appeared to influence the work reported in this paper.

Authors' contributions

Augusto Barbosa Silva: writing – original draft, visualization, conceptualization, formal analysis, investigation, methodology, data curation. José Wilson dos Santos Ferreira: writing – review & editing, visualization, supervision, project administration, validation, data curation. André Luís Brasil Cavalcante: visualization, supervision, resources, validation. Michéle Dal Toé Casagrande: writing – review & editing, visualization, supervision, resources, project administration, validation, data curation.

Data availability

The datasets generated and/or analyzed during the current study are not publicly available as they form part of an ongoing Ph.D. research project by Augusto Barbosa Silva, pending thesis defense. However, the data are available from the corresponding author upon reasonable request.

Declaration of use of generative artificial intelligence

ChatGPT (OpenAI) was used to assist with English language editing, including spelling revision and the translation of technical terminology. The authors take full responsibility for the content of the manuscript.

List of symbols and abbreviations

pH	potential of hydrogen
wt%	weight percentage
A	water absorption
Al	aluminum
ASTM	American Society for Testing and Materials
ATR	Attenuated Total Reflectance
Ca	calcium
CI	cellulose crystallinity index
COP30	30th Conference of the Parties
CNPq	Brazilian National Council for Scientific and Technological Development
Cr	chromium
Cu	copper
CuKα	copper K-alpha radiation
C–H	carbon-hydrogen bond
C=C	carbon-carbon double bond
C=O	carbonyl group
Df	fiber diameter
DTG	derivative thermogravimetry
EMBRAPA	Brazilian Agricultural Research Corporation
EVA	ethylene vinyl acetate
FAP/DF	Research Support Foundation of the Federal District
Fe	iron
FTIR	Fourier Transform Infrared Spectroscopy
IBGE	Brazilian Institute of Geography and Statistics
H_2O	water
H_2SO_4	sulfuric acid
K	potassium
KCl	potassium chloride
Lf	fiber length
LUDOX	colloidal silica trademark
Mn	manganese
NF	natural fiber
O–H	hydroxyl group
P	phosphorus
S	sulfur
SCDOT	South Carolina Department of Transportation
SEI-GDF	Secretariat of Economy of the Federal District, Brazil
SEM	scanning electron microscopy
Si	silicon
Si–O	cellulose – siloxane linkage with cellulose
SiO_2	silica
TGA	thermogravimetric analysis
Ti	titanium
TM-50 LUDOX	product grade
WF	waterproofed fiber
XRF	X-ray fluorescence
Zn	zinc
ΔpH	variation of pH
θ	diffraction angle (degrees)

References

Abu Qamar, M.I., & Suleiman, M.T. (2022). Evaluating the influence of surface roughness on interface shear strength of cohesive soil–structure interface subjected to axial monotonic loading. *Geo-Congress*, *2022*, 281-291. https://doi.org/10.1061/9780784484029.028.

Ali, A., Shaker, K., Nawab, Y., Jabbar, M., Hussain, T., Militky, J., & Baheti, V. (2016). Hydrophobic treatment of natural fibers and their composites: A review. *Journal of Industrial Textiles*, *47*(8), 2153-2183. https://doi.org/10.1177/1528083716654468.

Almeida, A.V. C., Melo, I.M., Pinheiro, I.S., Freitas, J.F., & Melo, A.C.S. (2017). Revalorização do caroço de açaí em uma beneficiadora de polpas do município de Ananindeua/PA: proposta de estruturação de um canal reverso orientado pela PNRS e logística reversa. GEPROS. Gestão da Produção. *Operações e Sistemas*, *12*(3), 59. https://doi.org/10.15675/gepros.v12i3.1668.

ASTM C1557. (2020). *Standard test method for tensile strength and Young's modulus of fibers*. ASTM International, West Conshohocken, PA. https://doi.org/10.1520/C1557-20.

ASTM D2974-20e1. (2023a). *Standard test methods for moisture, ash, and organic matter of peat and other organic soils*. ASTM International, West Conshohocken, PA. https://doi.org/10.1520/D2974-20E01.

ASTM D5550-23. (2023b). *Standard test method for specific gravity of soil solids by gas pycnometer*. ASTM International, West Conshohocken, PA. https://doi.org/10.1520/D5550-23.

Azevedo, A.R.G., Marvila, M.T., Tayeh, B.A., Cecchin, D., Pereira, A.C., & Monteiro, S.N. (2021). Technological performance of açaí natural fibre reinforced cement-based mortars. *Journal of Building Engineering*, *33*, 101675. https://doi.org/10.1016/j.jobe.2020.101675.

Bai, Y., Arulrajah, A., Horpibulsuk, S., & Chu, J. (2023). Gasified olive stone biochar as a green construction fill material. *Construction & Building Materials*, *403*, 133003. https://doi.org/10.1016/j.conbuildmat.2023.133003.

Balboni, B.M., de Sousa, J.T.R., Ferreira, M.A., Rodrigues, R.A., & Macedo, A.B. (2019). Residue of açaí berry (Euterpe oleracea) management as a source of lignocellulosic material. *Holz als Roh- und Werkstoff*, *77*(4), 509-516. https://doi.org/10.1007/s00107-019-01417-8.

Bilcati, G.K., Matoski, A., Trianoski, R., & Lengowski, E.C. (2018). Effects of pre-treatment of Curauá fibers on compatibility with portland cements. *Matéria (Rio de Janeiro)*, *23*(3), e12190. https://doi.org/10.1590/s1517-707620180003.0524.

Bordoloi, S., Garg, A., & Sekharan, S. (2017). A review of physio-biochemical properties of natural fibers and their application in soil reinforcement. *Advances in Civil Engineering Materials*, *35*(6), 2615-2634. https://doi.org/10.1520/ACEM20160076.

Boudali, S., Abdulsalam, B., Soliman, A., Poncet, S., Godbout, S., Palacios, J., & ElSafty, A. (2022). Implementation of agricultural crop wastes toward green construction materials. In F. Colangelo, R. Cioffi & I. Farina (Eds.), *Handbook of sustainable concrete and industrial waste management: recycled and artificial aggregate, innovative eco-friendly binders, and life cycle assessment* (pp. 305-332). Woodhead Publishing. https://doi.org/10.1016/B978-0-12-821730-6.00022-X.

Bufalino, L., Guimarães, A.A., Silva, B.M.S., Souza, R.L.F., Melo, I.C.N.A., Oliveira, D.N.P.S., & Trugilho, P.F. (2018). Local variability of yield and physical properties of açaí waste and improvement of its energetic attributes by separation of lignocellulosic fibers and seeds. *Journal of Renewable and Sustainable Energy*, *10*(5), 053102. https://doi.org/10.1063/1.5027232.

Buratto, R.T., Cocero, M.J., & Martín, Á. (2021). Characterization of industrial açaí pulp residues and valorization by microwave-assisted extraction. *Chemical Engineering and Processing*, *160*, 108269. https://doi.org/10.1016/j.cep.2020.108269.

Castro, C.L., Soares, A.B., & Aguiar, M.F.P. (2022). Soil–water characteristic curve of polypropylene fibre-reinforced sandy soil. *Soils and Rocks*, *45*(3), e2022070021. https://doi.org/10.28927/SR.2022.070021.

Crippa, M.T., Vendrame, P.R.S., Ferreira, J.W.S., & Teixeira, R.S. (2025). Hydro-mechanical behavior of tropical soils reinforced with recycled PET fibers: influence of weathering on fiber-matrix interaction. *Geotechnical and Geological Engineering*, *43*(2), 91. https://doi.org/10.1007/s10706-024-03061-3.

Cruz, J., & Fangueiro, R. (2016). Surface modification of natural fibers: A review. *Procedia Engineering*, *155*, 285-288. https://doi.org/10.1016/j.proeng.2016.08.030.

de Oliveira, D.N.P.S., Claro, P.I.C., de Freitas, R.R., Martins, M.A., Souza, T.M., Silva, B.M.S., Mendes, L.M., & Bufalino, L. (2019). Enhancement of the Amazonian açaí waste fibers through variations of alkali pretreatment parameters. *Chemistry & Biodiversity*, 16, e1900275. https://doi.org/10.1002/cbdv.201900275.

Eleutério, T., Trota, M.J., Meirelles, M.G., & Vasconcelos, H.C. (2025). A review of natural fibers: classification, composition, extraction, treatments, and applications. *Fibers*, *13*(9), 119. https://doi.org/10.3390/fib13090119.

El-Shekeil, Y.A., Sapuan, S.M., Khalina, A., Zainudin, E.S., & Al-Shuia'a, O.M. (2012). Effect of alkali treatment on mechanical and thermal properties of Kenaf fiber-reinforced thermoplastic polyurethane composite. *Journal of Thermal Analysis and Calorimetry*, *109*(3), 1435-1443. https://doi.org/10.1007/s10973-012-2258-x.

Garat, W., Corn, S., Le Moigne, N., Beaugrand, J., & Bergeret, A. (2018). Analysis of the morphometric variations in natural fibres by automated laser scanning: towards an efficient and reliable assessment of the cross-sectional area. *Composites. Part A, Applied Science and Manufacturing*, *108*, 114-123. https://doi.org/10.1016/j.compositesa.2018.02.018.

Gessner, M.O. (2005). Proximate lignin and cellulose. In M.A. Graça, F. Bärlocher & M.O. Gessner (Eds.), *Methods to Study Litter Decomposition: a practical guide*. Dordrecht: Springer. https://doi.org/10.1007/1-4020-3466-0_17.

Guarino, V., Caputo, T., Altobelli, R., & Ambrosio, L. (2015). Degradation properties and metabolic activity of alginate and chitosan polyelectrolytes for drug delivery and tissue engineering applications. *AIMS Materials Science*, *2*(4), 497-502. https://doi.org/10.3934/matersci.2015.4.497.

Han, F., Ganju, E., Salgado, R., & Prezzi, M. (2018). Effects of interface roughness, particle geometry, and gradation on the sand–steel interface friction angle. *Journal of Geotechnical and Geoenvironmental Engineering*, *144*(12), 04018096. https://doi.org/10.1061/(ASCE)GT.1943-5606.0001990.

Hasan, K.M.F., Horváth, P.G., Bak, M., & Alpár, T. (2021). A state-of-the-art review on coir fiber-reinforced biocomposites. *RSC Advances*, *11*(18), 10548-10571. https://doi.org/10.1039/D1RA00231G.

Hasanzadeh, M., Shahriyari Far, H., Haji, A., & Rosace, G. (2022). Surface modification of polyester/viscose fabric with silica hydrosol and amino-functionalized polydimethylsiloxane for the preparation of a fluorine-free superhydrophobic and breathable textile. *Coatings*, *12*(3), 398. https://doi.org/10.3390/coatings12030398.

Hassanpour, B., & Karbhari, V.M. (2024). Characteristics and models of moisture uptake in fiber-reinforced composites: A topical review. *Polymers*, *16*(16), 2265. https://doi.org/10.3390/polym16162265.

Huang, Y., Sultan, M.T.H., Shahar, F.S., Łukaszevicz, A., Oksiuta, Z., & Grzelą, R. (2025). Kenaf fiber-reinforced biocomposites for marine applications: A review. *Materials*, *18*(5), 999. https://doi.org/10.3390/ma18050999.

Huzni, S., Ikramullah, I., Ibrahim, I.B.M., Fonna, S., Sukhairi, T.A., Afrizal, A., Muksin, U., Khalil, H.P.S.A., Aprilia, S., & Rizal, S. (2022). The role of typha angustifilia fiber–matrix bonding parameters on interfacial shear strength analysis. *Polymers*, *14*(5), 1006. https://doi.org/10.3390/polym14051006.

Instituto Brasileiro de Geografia e Estatística – IBGE. (2025). *Produção agropecuária: Açaí (cultivo)*. Retrieved in January 21, 2026, from https://www.ibge.gov.br/explica/producao-agropecuaria/acai-cultivo/br

Kadhim, H.K., & Alyounis, M. (2024). Effect of surface roughness on interface shear strength parameters of sandy soils. *Open Engineering*, *14*(1), 118-132. https://doi.org/10.1515/eng-2024-0018.

Kargarzadeh, H., Ahmad, I., Abdullah, I., Dufresne, A., Zainudin, S.Y., & Sheltami, R.M. (2012). Effects of hydrolysis conditions on the morphology, crystallinity, and thermal stability of cellulose nanocrystals. *Cellulose (London, England)*, *19*(3), 855-866. https://doi.org/10.1007/s10570-012-9684-6.

Leite-Barbosa, O., Pinto, C.C.D.O., Leite-da-Silva, J.M., de Aguiar, E.M.M.M., & Veiga-Junior, V.F. (2024). Polymer composites reinforced with residues from amazonian agro-extractivism and timber industries: a sustainable approach to enhancing material properties and promoting bioeconomy. *Polymers*, *16*(23), 3282. https://doi.org/10.3390/polym16233282.

Li, H., Yang, J., Wang, L., Zhang, N., Wang, Q., & Mechtcherine, V. (2024). Recycling of biomass combustion ash into SCMs and aggregates. In L. Wang, D. Tsang & J. Yan (Eds.), *Treatment and Utilization of Combustion and Incineration Residues* (pp. 269-295). Elsevier. https://doi.org/10.1016/B978-0-443-21536-0.00022-8.

Lima, A.C.P., Bastos, D.L.R., Camarena, M.A., Bon, E.P.S., Cammarota, M.C., Teixeira, R.S.S., & Gutarra, M.L.E. (2021). Physicochemical characterization of residual biomass (seed and fiber) from açaí (Euterpe oleracea) processing and assessment of the potential for energy production and bioproducts. *Biomass Conversion and Biorefinery*, *11*(3), 925-935. https://doi.org/10.1007/s13399-019-00551-w.

Liu, Y., Xie, J., Wu, N., Ma, Y., Menon, C., & Tong, J. (2019). Characterization of natural cellulose fiber from corn stalk waste subjected to different surface treatments. *Cellulose*, *26*(7), 4707-4719. https://doi.org/10.1007/s10570-019-02429-6.

Lopes, M.M., & Casagrande, M.D.T. (2022). Mechanical improvement of a reinforced sand with açaí (*Euterpe oleracea*). *IOP Conference Series. Materials Science and Engineering*, 1260(1), 012025. https://doi.org/10.1088/1757-899X/1260/1/012025.

Lv, C., He, P., Pang, G., & Liu, J. (2023). Effect of wet–dry cycling on properties of natural-cellulose-fiber-reinforced geopolymers: A short review. *Molecules (Basel, Switzerland)*, 28(20), 7189. https://doi.org/10.3390/molecules28207189.

Maia, M.T., Noronha, V.T., Oliveira, N.C., Alves, A.C., Faria, A.F., Martinez, D.T.S., Ferreira, O.P., & Paula, A.J. (2022). Silica nanoparticles and surface silanization for the fabrication of water-repellent cotton fibers. *ACS Applied Nano Materials*, 5(4), 4634-4647. https://doi.org/10.1021/acsanm.1c03346.

Martinelli, F.R.B., Ribeiro, F.R.C., Marvila, M.T., Monteiro, S.N., Filho, F.C.G., & Azevedo, A.R.G. (2023). A review of the use of coconut fiber in cement composites. *Polymers*, 15(5), 1309. https://doi.org/10.3390/polym15051309.

Martins, M.A., Pessoa, J.D.C., Gonçalves, P.S., Souza, F.I., & Mattoso, L.H.C. (2008). Thermal and mechanical properties of the açaí fiber/natural rubber composites. *Journal of Materials Science*, 43(21), 6531-6538. https://doi.org/10.1007/s10853-008-2842-4.

Marvila, M.T., Azevedo, A.R.G., Cecchin, D., Costa, J.M., Xavier, G.C., de Fátima do Carmo, D., & Monteiro, S.N. (2020). Durability of coating mortars containing açaí fibers. *Case Studies in Construction Materials*, 13, e00406. https://doi.org/10.1016/j.cscm.2020.e00406.

Mesquita, A.L. de L., Barrero, N.G., Fiorelli, J., Christoforo, A.L., De Faria, L.J.G., & Lahr, F.A.R. (2018). Eco-particleboard manufactured from chemically treated fibrous vascular tissue of acai (*Euterpe oleracea* Mart.) fruit: A new alternative for the particleboard industry with its potential application in civil construction and furniture. *Industrial Crops and Products*, *112*, 644-651. https://doi.org/10.1016/j.indcrop.2017.12.074.

Muñoz-Blandón, O., Ramírez-Carmona, M., Rendón-Castrillón, L., & Ocampo-López, C. (2023). Exploring the potential of fique fiber as a natural composite material: A comprehensive characterization study. *Polymers*, *15*(12), 2712. https://doi.org/10.3390/polym15122712.

Nasser, J., Lin, J., & Sodano, H. (2018). High strength fiber reinforced composites with surface fibrillized aramid fibers. *Journal of Applied Physics*, *124*(4), 045305. https://doi.org/10.1063/1.5026987.

Natalli, J.F., Pereira, I.S.A., Júnior, E.R.G., Malafaia, S.A.A., Batista, I.D., Barbosa, M.V., Marvila, M.T., Margem, F.M., Lima, T.E.S., Monteiro, S.N., & Azevedo, A.R.G. (2024). Performance evaluation of açaí fiber as reinforcement in coating mortars. In Z. Peng, A.R.G. Azevedo & S.N. Monteiro (Eds.), *Characterization of minerals, metals, and materials 2024* (pp. 587-596). Springer. https://doi.org/10.1007/978-3-031-50304-7_57.

Neto, J.S.S., Queiroz, H.F.M., Aguiar, R.A.A., & Banea, M.D. (2021). A review on the thermal characterisation of natural and hybrid fiber composites. *Polymers*, *13*(24), 4425. https://doi.org/10.3390/polym13244425.

Nguyen, T.T., & Indraratna, B. (2023). Natural fibre for geotechnical applications: concepts, achievements and challenges. *Sustainability*, *15*(11), 8603. https://doi.org/10.3390/su15118603.

Nguyen-Tri, P., Altiparmak, F., Nguyen, N., Tuduri, L., Ouellet-Plamondon, C.M., & Prud'homme, R.E. (2019). Robust superhydrophobic cotton fibers prepared by simple dip-coating approach using chemical and plasma-etching pretreatments. *ACS Omega*, *4*(4), 7829-7837. https://doi.org/10.1021/acsomega.9b00688.

Nurazzi, N.M., Asyraf, M.R.M., Rayung, M., Norrrahim, M.N.F., Shazleen, S.S., Rani, M.S.A., Shafi, A.A.R., Aisyah, H.M., Radzi, M.H.M., Sababuddin, F.A., Ilyas, R.A., Zainudin, E.S., & Abdan, K. (2021). Thermogravimetric analysis properties of cellulosic natural fiber polymer composites: A review on influence of chemical treatments. *Polymers*, *13*(16), 2710. https://doi.org/10.3390/polym13162710.

Oliveira, A.M., Oliveira, A.L.B., Silva, J.L.M., Marques, M.G.S., Vasconcelos, R.V., & Oliveira, D.R.C. (2020). Influência de tratamentos superficiais na absorção de água e na resistência à tração de fibras vegetais de Ureana lobata Linn. *Revista Tecnia*, *5*(1), e983. Retrieved in January 21, 2026, from https://periodicos.ifg.edu.br/tecnia/article/view/983

Oliveira, D.N.P.S., Matos, L.C., Souza, T.M., Aráujo, E.S., Silva, M.G., Cabral, C.P.T., Mendes, L.M., Rocha, Q.S., & Bufalino, L. (2024). Methods for separating the lignocellulosic fibers from the açaí pulping waste: quality for kraft pulping. *Cerne*, *30*, e-103376. http://dx.doi.org/10.1590/01047760202430013376.

Oun, A., Manalo, A., Alajarmeh, O., Abousnina, R., & Gerdes, A. (2022). Long-term water absorption of hybrid flax fibre-reinforced epoxy composites with graphene and its influence on mechanical properties. *Polymers*, *14*(17), 3679. https://doi.org/10.3390/polym14173679.

Pathak, B., Yin, Z.-Y., Fu, Y., & Luo, Z. (2025). Evolution of surface roughness and particle breakage with interface shear behaviour of sand-epoxied GFRP against sand under elevated normal stress. *Canadian Geotechnical Journal*, *62*, 1-28. https://doi.org/10.1139/cgj-2025-0327.

Pessoa, J.D.C., Arduin, M., Martins, M.A., & de Carvalho, J.E.U. (2010). Characterization of Açaí (E. oleracea) fruits and its processing residues. *Brazilian Archives of Biology and Technology*, *53*(6), 1451-1460. https://doi.org/10.1590/S1516-89132010000600022.

Pickering, K.L., Efendy, M.G.A., & Le, T.M. (2016). A review of recent developments in natural fibre composites and their mechanical performance. *Composites. Part A, Applied Science and Manufacturing*, *83*, 98-112. https://doi.org/10.1016/j.compositesa.2015.08.038.

Poletto, M., Ornaghi Júnior, H.L., & Zattera, A.J. (2014). Native cellulose: Structure, characterization and thermal properties. *Materials*, *7*(9), 6105-6119. https://doi.org/10.3390/ma7096105.

Polidori, G., Murer, S., Beaumont, F., Lachi, M., Bliard, C., Nait-Rabah, O., Bufalino, L., & Bogard, F. (2024). An update on the waste management of the Amazonian açaí berry for the civil engineering sector. *Sustainability*, *16*(19), 8451. https://doi.org/10.3390/su16198451.

Radzuan, N.A.M., Tholibon, D., Sulong, A.B., Muhamad, N., & Che Haron, C.H. (2020). Effects of high-temperature exposure on the mechanical properties of kenaf composites. *Polymers*, *12*(8), 1643. https://doi.org/10.3390/polym12081643.

Rocha, D.L., Tambara Júnior, L.U.D., Marvila, M.T., Pereira, E.C., Souza, D., & de Azevedo, A.R.G. (2022). A review of the use of natural fibers in cement composites: Concepts, applications and Brazilian history. *Polymers*, *14*(10), 2043. https://doi.org/10.3390/polym14102043.

Santos, G.Z.B., Caldas, L.R., Melo Filho, J.A., Rafael, S.I.M., & Silva, N.M. (2022). Environmental performance of a cement composite reinforced with vegetable fibers cultivated in the Brazilian Amazon. *Cleaner and Circular Bioeconomy*, *3*, 100034. https://doi.org/10.1016/j.clcb.2022.100034.

Sato, M.K., de Lima, H.V., Costa, A.N., Rodrigues, S., Pedroso, A.J.S., & de Freitas Maia, C.M.B. (2019). Biochar from Acai agroindustry waste: study of pyrolysis conditions. *Waste Management*, *96*, 158-167. https://doi.org/10.1016/j.wasman.2019.07.022.

Schneider, C.A., Rasband, W.S., & Eliceiri, K.W. (2012). NIH Image to ImageJ: 25 years of image analysis. *Nature Methods*, *9*(7), 671-675. https://doi.org/10.1038/nmeth.2089.

Segal, L., Creely, J.J., Martin Junior, A.E., & Conrad, C.M. (1959). An empirical method for estimating the degree of crystallinity of native cellulose using the X-ray diffractometer. *Textile Research Journal*, *29*(10), 786-794. https://doi.org/10.1177/004051755902901003.

Shifa, S.S., Kanok, M.M.H., & Haque, M.S. (2024). Effect of alkali treatment on mechanical and water absorption properties of biodegradable wheat-straw/glass fiber reinforced epoxy hybrid composites. *Heliyon*, *10*(16), e35910. https://doi.org/10.1016/j.heliyon.2024.e35910.

Signorini, C., Nobili, A., Cedillo González, E.I., & Siligardi, C. (2018). Silica coating for interphase bond enhancement of carbon and AR-glass textile reinforced mortar (TRM). *Composites. Part B, Engineering*, *141*, 191-202. https://doi.org/10.1016/j.compositesb.2017.12.045.

Silveira, M.V., Ferreira, J.W.S., & Casagrande, M.D.T. (2022). Effect of surface treatment on natural aging and mechanical behavior of sisal fiber–reinforced sand composite. *Journal of Materials in Civil Engineering*, *34*(6), 06022001. https://doi.org/10.1061/(ASCE)MT.1943-5533.0004237.

South Carolina Department of Transportation – SCDOT. (2022). *Geotechnical Design Manual (GDM)*. Retrieved in January 21, 2026, from https://www.scdot.org/business/geotech.html

Tavares, F.F.C., Almeida, M.D.C., Silva, J.A.P., Araújo, L.L., Cardozo, N.S.M., & Santana, R.M.C. (2020). Thermal treatment of açaí (Euterpe oleracea) fiber for composite reinforcement. *Polímeros*, *30*(1), e2020003. https://doi.org/10.1590/0104-1428.09819.

Teixeira, P.C., Donagemma, G.K., Fontana, A., & Teixeira, W.G. (2017). *Manual de métodos de análise de solo* (3. ed.). Embrapa. Retrieved in January 21, 2026, from https://www.infoteca.cnptia.embrapa.br/handle/doc/1085209

Vincenzini, A., Augarde, C.E., & Gioffrè, M. (2021). Experimental characterization of natural fibre–soil interaction: lessons for earthen construction. *Materials and Structures*, *54*(3), 110. https://doi.org/10.1617/s11527-021-01703-z.

Zhang, X., Liu, X., Wang, G., Xu, Y., & Gao, H. (2025). Causes of the high friction angle of diatomaceous soil: microscale and nanoscale insights. *Geotechnique*, *75*(3), 362-378. https://doi.org/10.1680/jgeot.23.00230.

Zhang, Y.M., Zhao, Q., Li, L., Yan, R., Zhang, J., Duan, C.J., Liu, B.J., Sun, Z.Y., Zhang, M.Y., Hu, W., & Zhang, N.N. (2018). Synthesis of a lignin-based phosphorus-containing flame retardant and its application in polyurethane. *RSC Advances*, *8*(56), 32252-32261. https://doi.org/10.1039/C8RA05598J.

Zhu, C., Wang, B., Meng, J., Deng, S., Fan, X., Peng, T., Zhou, W., Li, Y., Li, H., & Zhao, C. (2019). Surface modification of PBO fiber by grafting nanoporous SiO_2 coating with improved interfacial properties. *Materials Research Express*, *6*(9), 095317. https://doi.org/10.1088/2053-1591/ab3096.